*33rd EPS Conference on Plasma Phys. Rome, 19 - 23 June 2006 ECA Vol.**30I**, P-5.158 (2006)*

Coherent structures in sheared velocity flow.

Åshild Fredriksen[1], Claudia Riccardi[2], H. Eduardo Roman[2], and Ruggero Barni[2]

[1]*Dep. Physics, University of Tromsø, N-9037 Tromsø, Norway*

[2]*Dep. Physics, University of Milano-Bicocca and INFM, 20126 Milano, Italy*

1. OBSERVATIONS OF SHEARED FLOWS IN BLAAMANN AND IMPACT ON COHERENT STRUCTURES

In the simple magnetized torus Blaamann, coherent structures are known to exist, and their features are reported in previous papers [1, 2]. Monopolar and dipolar structures are rotating in the poloidal cross-section with ExB velocity. Generally, in Blaamann, the plasma is rotating like a rigid body in most of the cross- section. However, in some localized regions a strong velocity shear is present. Fig. 1 shows a color plot of the absolute values of the velocity shear. While the largest shear values along the rim is due to the plasma-wall sheath, the slightly weaker shear region in the upper left quarter of the cross-section is interior to the plasma. This shear region induces a constriction in the flow 'channel' between the filament region in the middle and the outer rim. The line contours plotted onto the color-coded shear plot, depict the time frame of the 2D conditionally averaged fluctuations [1, 2] in the electron saturation current (ESC), taken at time lag τ = -16 μsec with respect to the minimum of an average negative floating potential structure on the reference probe. (The condition to pick a structure is that its amplitude is more negative than -1.5 σ, σ being the standard deviation.) The plot illustrates how positive and negative vortical structures in the

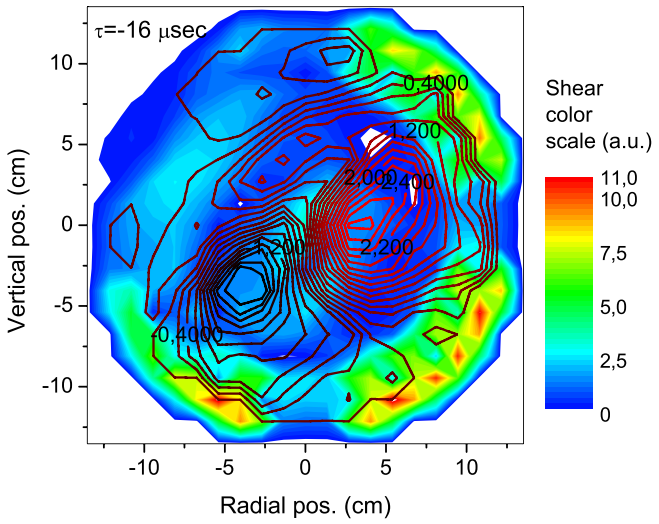

Figure 1. Absolute value of velocity shear derived from average plasma potential in color plot. Low value structures along the rim are artifacts from the derivative of $V_{ExB.}$ Overlayed line contour plot is the conditionally averaged fluctuations in the electron saturation current taken 16 ms prior to the condition fulfilled at reference probe. Red lines correspond to positive structure.

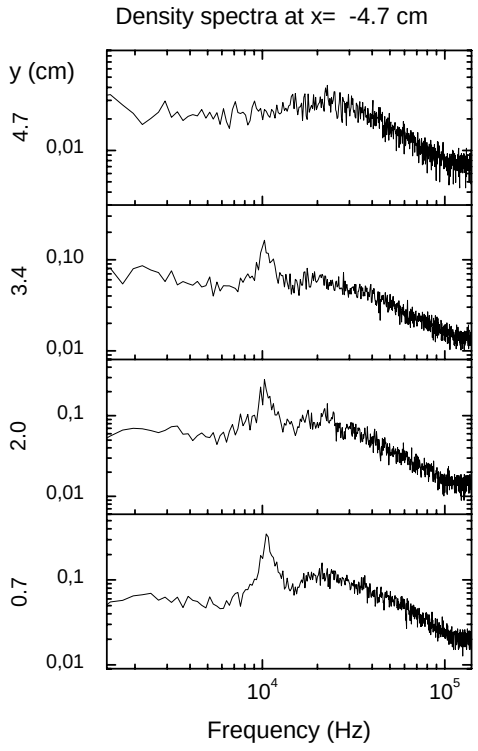

Figure 2. Power spectra of fluctuations in the electron saturation current, taken at radial position -4.7 cm and four vertical positions, from 0.7 to 4.7 cm

density fluctuations propagate away from the velocity shear, ie. in the regions with constant background velocity, while they are strongly damped and partially fragmented across the shear. This is also evidenced in the power spectra of the density fluctuations. In Fig. 2, spectra at x=-4.7cm and at four different vertical positions are shown. The spectra at y=0.7, 2.0, and 3.4 cm are all outside the shear boundary (on the low-field side), and they all feature a prominent peak at about 10 kHz, providing signatures of coherent structures with a periodicity of ~100 μsec, as previously reported in [2]. On the other hand, the y= 4.7 cm position is situated in a region of maximum shear, and here the peak in the spectrum has vanished, leaving only the features of developed turbulence. Looking at statistical moments of the fluctuations, we observed low variance, negative skewness, and high kurtosis values across and towards the high-field side of the shear region. In this work, we will focus our attention on the analysis of the dynamical evolution of the structures in the presence of sheared flow regions.

2. STATISTICAL ANALYSIS

Statistical analysis suggests, according to numerical papers [3], that vortical structures are stretched and fragmented into smaller scale structures in the proximity of sheared velocity regions. Here we apply a percolation-type of cluster analysis to obtain statistics of their size, position, and polarity. Also, information on rotational speed was obtained with this analysis. As a starting point of the analysis, 8 μsec resolution time frames of average structures in the electron saturation current were obtained by standard conditional averaging technique [1]. In Fig. 3, the time frame at τ= -16 μsec has been sorted into positive (full red squares) and negative (open blue squares) values of the ESC, each representing one probe position, called a site. There are 225 sites in the full poloidal plane. A cluster of sites is

defined as the structure of connected sites having the same sign. Two sites are said to be connected if they are nearest neighbour to each other.

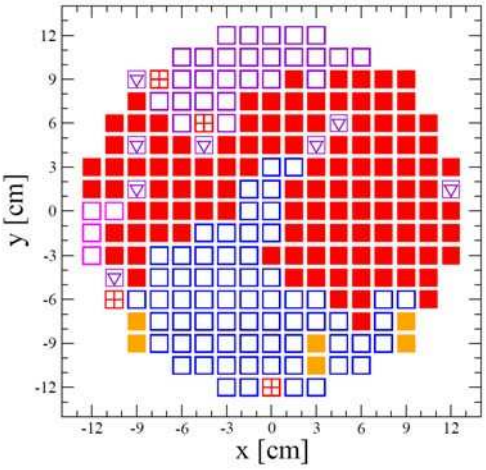

Figure 3. The frame at t= -16 μsec for the conditional sampling of ESC fluctuations in Blaamann. The squares represent the positions (in normalized units) on the poloidal plane. The full (red) squares correspond to positive ESC values, while the open (blue) ones to negative ones. Single positive sites are indicated with a +, while single negative ones with a triangle down symbol.

Applying a percolation-type of cluster enumeration (see e.g. [5]), we identify all the clusters present in the poloidal plane for each temporal frame. We can thus perform a statistical analysis of their spatial extensions and locations. When sorting the clusters by size, we found for both positive and negative clusters separately, that the largest cluster exceeded the second largest in size by more than a factor four for the positive structures, and by the same factor between -80 and +240 μsec for the negative ones. Fig. 4 depicts the center of mass of the positive clusters for all the time frames. It is evident from the Figure that the largest clusters are closer to the center of the plane. On the other hand, the fragmented clusters are located closer to the rim, where they accumulate preferentially in the shear region x<0, y>0 on the high-field side of the shear layer, after the main structure is being stretched in the shear. A similar, but less clear result was found for the negative clusters.

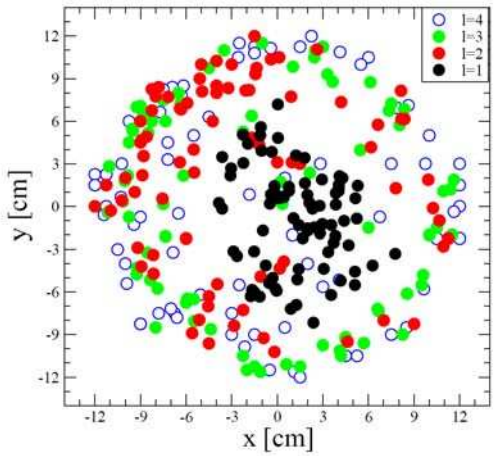

Figure 4. The positions of the center of mass (circles) for the largest four positive clusters for all the temporal frames. The l=1 indicates the largest cluster (black), l=2 the 2nd largest, and so on.

By relating the cluster size, denoted as N_i, to the background velocity given by

$$\overline{v}_i = \frac{1}{N_i}\sum_{j=1}^{N_i} v_j$$

we can investigate whether the positioning of the structures are related to the velocity of the clusters.We find that for the larger cluster sizes, say for $Ni > 70$, the values of $\overline{v}_i$ tends on average to be small, while for small cluster sizes, e.g. $N_i < 50$, $\overline{v}_i$ is significantly larger.

Finally, we calculate the rotational speed of the signal, by finding the 'dipole' moment of the signal according to, $p_x = \frac{1}{N}\sum_{j=1}^{N} x_j S_j$ $p_y = \frac{1}{N}\sum_{j=1}^{N} y_j S_j$

Where S_j is the value of the ESC fluctuation at site j with coordinates (x_j, y_j) and N=225. Since, by definition, $p_x = p\cos(\phi)$, $p_y = p\sin(\phi)$, where $p = \sqrt{p_x^2 + p_y^2}$, we can determine the temporal evolution of the phase velocity $\dot{\phi}$. The results are plotted in Fig. 5 in the form of a phase portrait, i.e. p_y versus p_x, which displays clearly the rotational character of the coherent fluctuations. In Fig. 6, we plot the actual phase velocity $\dot{\phi}$ as a function of the temporal frame. One can see that for frames in the range $25 < j < 65$ the mode rotates with an approximately constant speed ≈ 0.5 [rad/frame], ie. ~10 kHz, which is the frequency also seen in the spectra.

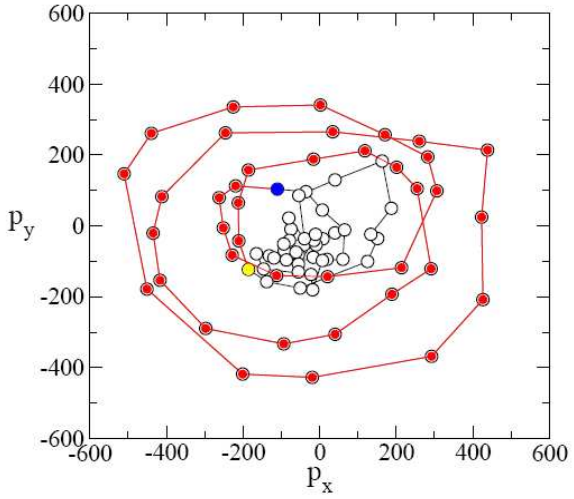

Figure 5 Dipole moments diagram plotted as p_y vs p_x for the 80 temporal frames of the conditional sampling images (circles). The red circles indicate temporal frames in the range $25 < j < 65$, corresponding to rotational speeds which are roughly constant (see Fig. 6). The blue circle corresponds to the 25th frame, and the yellow one to the 65th one.

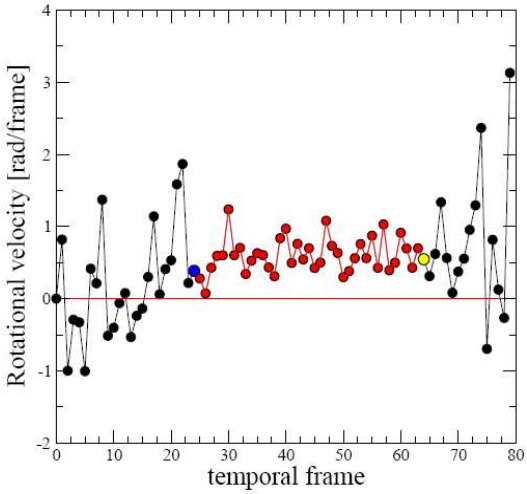

Figure 6 The phase velocity of the dipole moment of the image $\dot{\phi}$ [rad/frame] as a function of temporal frame.

3. References.

1. Øynes et al, Phys. Rev. E 57 (1995) 2242
2. Fredriksen et al., Plasma Phys. Contr. Fusion 45 (2003) 721
3. Krane et al., Phys. Rev. Lett. 80 (1998) 4422
4. A. Bunde and S. Havlin (eds.), 'Fractals and Disordered Systems', 2nd edition, Springer, Heidelberg, 1996.